Indonesian Journal of Cardiology
Indonesian J Cardiol • Vol. 47 • 2026
pISSN: 2830-3105 / eISSN: 2964-7304
doi: 10.30701/ijc.2194

Original Article

Development of an Early-Stage Diabetic Cardiomyopathy Rat Model with Early Myocardial Remodeling Induced by HFHF Diet and Low-Dose Streptozotocin

Susetyo Atmojo[1,2], Bambang Budi Siswanto[1,2,3], Nurjati Chairani Siregar[1,4,5], Aria Kekalih[6], Fadlina Chany Saputri[7], Budi Susetyo Pikir[8,9], Deni Noviana[10], Khanisyah Erza Gumilar[11], Puspita Eka Wuyung[1,4,12]

[1] Doctoral Program in Medical Sciences, Faculty of Medicine, Universitas Indonesia, Jakarta, Indonesia.
[2] National Cardiovascular Center Harapan Kita, Jakarta, Indonesia.
[3] Department of Cardiology and Vascular Medicine, Faculty of Medicine, Universitas Indonesia, Jakarta, Indonesia.
[4] Department of Anatomical Pathology, Faculty of Medicine, Universitas Indonesia, Jakarta, Indonesia.
[5] Dr. Cipto Mangunkusumo General Hospital, Jakarta, Indonesia
[6] Department of Community Medicine, Faculty of Medicine, Universitas Indonesia, Jakarta, Indonesia
[7] Department of Pharmacology-Toxicology, Faculty of Pharmacy, Universitas Indonesia, Jakarta, Indonesia
[8] Department of Cardiology and Vascular Medicine, Faculty of Medicine, Universitas Airlangga, Surabaya, Indonesia
[9] Dr. Soetomo General Academic Hospital – Universitas Airlangga Hospital, Surabaya, Indonesia
[10] Division of Surgery and Radiology, School of Veterinary Medicine and Biomedical Sciences, IPB University, Bogor, Indonesia
[11] Department of Obstetrics and Gynecology, Faculty of Medicine, Universitas Airlangga, Surabaya, Indonesia
[12] Animal Research Facility, IMERI, Faculty of Medicine, Universitas Indonesia, Jakarta, Indonesia

Correspondence:
Susetyo Atmojo,

Doctoral Program in Medical Sciences, Faculty of Medicine, Universitas Indonesia/ National Cardiovascular Center Harapan Kita, Jakarta, Indonesia.

Email: susetyo.atmojo@gmail.com

Abstract

Background: Diabetic Cardiomyopathy (DCM) is defined as structural and functional abnormalities of the myocardium occurring in individuals with Diabetes Mellitus (DM) in the absence of other conventional cardiovascular risk factors. Establishing a reliable early-stage DCM model is essential for mechanistic studies and therapeutic evaluation. This study aimed to characterize an early-stage DCM model in male Sprague–Dawley rats using a High-Fat High-Fructose (HFHF) diet combined with low-dose Streptozotocin (STZ).

Methods: Twelve male Sprague–Dawley rats (7–8 weeks, 200–250 g) were randomly assigned to three groups (n=4/group): control, HFHF + STZ 25 mg/kg, and HFHF + STZ 40 mg/kg. Rats received an HFHF diet for 12 weeks, followed by intraperitoneal STZ induction. Fasting blood glucose, lipid profile, cardiac echocardiography, serum N-Terminal pro-B-type Natriuretic Peptide (NT-proBNP), and myocardial histopathology were assessed. Data were analyzed using ANOVA or Kruskal–Wallis as appropriate.

Results: Both STZ doses induced persistent hyperglycemia without significant body-weight changes, consistent with a DCM metabolic phenotype. NT-proBNP levels were significantly elevated in both STZ groups compared with controls ($p<0.05$), indicating early myocardial stress despite preserved systolic and diastolic function on echocardiography. Histopathological evaluation showed increased inflammatory cell infiltration and progressive fibrosis in the HFHF+STZ groups, with a graded pattern across STZ doses.

Conclusions: The combination of an HFHF diet and low-dose STZ reproduced an early-stage DCM model characterized by persistent hyperglycemia, elevated NT-proBNP, and early myocardial remodeling while cardiac function remains preserved. This model reflects early DCM and is suitable for mechanistic studies and for testing therapies aimed at preventing progression to advanced myocardial dysfunction.

Keywords: Diabetic Cardiomyopathy, High-Fat High-Fructose Diet, Streptozotocin.

Introduction

Diabetes Mellitus (DM) is a chronic metabolic disorder characterized by elevated blood glucose levels.[1] Its global incidence and prevalence continue to rise, with an estimated 537 million adults affected in 2021 and the number projected to reach 783 million by 2045.[2-3] This growing burden contributes substantially to increased morbidity and mortality worldwide.[4-5] Cardiovascular complications are among the most significant consequences of DM, conferring a two- to four-fold higher risk of cardiovascular disease in adults compared with individuals without DM.[6-7] Heart failure is one of the most frequent and severe cardiovascular complications and remains a leading cause of death in patients with type 2 diabetes,[8] often occurring independently of atherosclerosis or other traditional risk factors.[9-10] This condition progresses into Diabetic Cardiomyopathy (DCM), defined as structural and/or functional abnormalities of the myocardium in patients with DM in the absence of other identifiable causes of myocardial dysfunction, such as coronary artery disease, hypertension, valvular disease, or congenital heart defects.[11-12] The pathogenesis of DCM is highly complex, involving chronic inflammation, cardiomyocyte apoptosis, and myocardial fibrosis driven by persistent hyperglycemia and metabolic stress.[13-14] These processes lead to progressive structural and functional alterations in the heart, including ventricular systolic and diastolic dysfunction, ultimately culminating in heart failure.[11-13]

The development of animal models of DCM aims to generate diabetic conditions accompanied by structural alterations of the myocardium, with or without clinically evident cardiac dysfunction. Most DCM animal models exhibit structural changes that resemble those observed in humans.[15] Translational research on DCM is essential for elucidating the fundamental mechanisms underlying myocardial dysfunction in diabetes, thereby enabling the development of therapeutic strategies that specifically target its root pathophysiology. Given the numerous confounding factors in human populations (such as lifestyle, obesity, hypertension, and medication use), animal models offer tighter control of variables and allow experimental manipulation to establish causal relationships. Streptozotocin (STZ)-based diabetes models provide functional, molecular, and cellular characteristics that are consistent with the features of DCM.[16]

Several experimental models have been developed to investigate DCM, including diet-induced models, chemically induced models, combined diet–STZ models, and genetic models. Each model reproduces different aspects of human DCM with distinct strengths and limitations regarding insulin resistance, β-cell dysfunction, and myocardial remodeling. Diet-only models primarily mimic metabolic syndrome but often require prolonged feeding to induce consistent cardiac remodeling, whereas the addition of low-dose STZ accelerates hyperglycemia through partial β-cell dysfunction while preserving key features of Type 2 Diabetes Mellitus (T2DM). Despite these advances, considerable variability remains in dietary composition, STZ dosage, and disease severity, highlighting the need for further characterization of reproducible early-stage DCM models for mechanistic and therapeutic studies.[17–20]

Among these experimental approaches, the combination of a High-Fat Diet (HFD) and STZ administration is commonly referred to as the fat-fed STZ model. A HFD induces insulin resistance through leptin signaling disruption and obesogenic processes, whereas STZ injection causes partial destruction of pancreatic β-cells.[4] Several studies have reported that administering high-fat or high-calorie diets for 4–8 weeks followed by intraperitoneal STZ injection (the "two-hit" approach) can generate a T2DM model with more pronounced disease progression.[21]

In this initial study, we used a High-Fat, High-Fructose (HFHF) diet combined with low-dose STZ to better replicate the metabolic milieu of T2DM and characterize early myocardial injury. This strategy was designed to detect subclinical myocardial stress using N-Terminal pro-B-type Natriuretic Peptide (NT-proBNP) as an early predictive biomarker and to identify structural remodeling before echocardiography detects functional impairment. This early-stage phenotype provides a translationally relevant platform for evaluating interventions aimed at modifying myocardial remodeling before irreversible dysfunction develops. Therefore, this study aimed to characterize and compare two low-dose STZ regimens (25 and 40 mg/kg) following 12 weeks of HFHF feeding to establish a reproducible early-stage DCM phenotype suitable for mechanistic and therapeutic studies.

Methods

Ethical Approval

All animal procedures were conducted in accordance with institutional animal care guidelines and were approved by the Health Research Ethics

Committee of Dr. Cipto Mangunkusumo National General Hospital – Faculty of Medicine, Universitas Indonesia (Approval No. KET-231/UN2.F1/ETIK/PPM.00.02/2025).

Study Period and Location

This pilot experimental study was conducted between March and July 2025 at the Animal Research Facility, IMERI, Faculty of Medicine, Universitas Indonesia, Jakarta, Indonesia. All animal housing and experimental procedures were performed at this facility. Echocardiographic assessments were conducted at the veterinary cardiology unit, and laboratory analyses including biochemical assays and ELISA measurements were performed at the integrated biomedical laboratory of the Faculty of Medicine, Universitas Indonesia.

Experimental Design

Study Animals and Population Determination

A total of twelve male Sprague–Dawley rats aged 7–8 weeks and weighing 200–250 g were used in this study. The sample size (n = 4 per group) was determined based on the exploratory nature of this pilot study, which aimed to identify early-stage myocardial remodeling trends (Figure 1).

Housing and Animal Welfare

Animals were housed in plastic cages under controlled environmental conditions with a 12:12-hour light–dark cycle and free access to food and water. All procedures complied with institutional guidelines for animal care and use. Rats underwent a one-week acclimatization period before intervention.

Group Allocation and Intervention

Rats were randomly allocated into three groups using simple randomization: The control group received standard chow without STZ induction, whereas the treatment groups received an HFHF diet combined with STZ induction at doses of 25 mg/kgBW or 40 mg/kgBW.

The HFHF diet consisted of pellet feed containing 458.32 kcal/100 g (32.48% fat, 10.70% protein, 51.05% carbohydrates) obtained from Brawijaya University, Malang, Indonesia.

The high-fructose component was administered as a 55% fructose solution via intragastric gavage at 1.5 mL twice daily for 12 weeks.

STZ Induction

After 12 weeks of dietary intervention, STZ was administered intraperitoneally following 6–7 hours of fasting. STZ was freshly dissolved in 0.1 M citrate buffer (pH 4.5) and injected within 5 minutes of preparation. Rats were considered diabetic when fasting blood glucose consistently reached ≥200 mg/dL within 3–7 days post-induction.

Euthanasia and Tissue Collection

At week 16 (four weeks after STZ injection), rats were fasted for 12 hours and anesthetized using ketamine–xylazine prior to blood collection and necropsy. Hearts were excised and fixed in 10% formalin for 24 hours for histopathological processing.

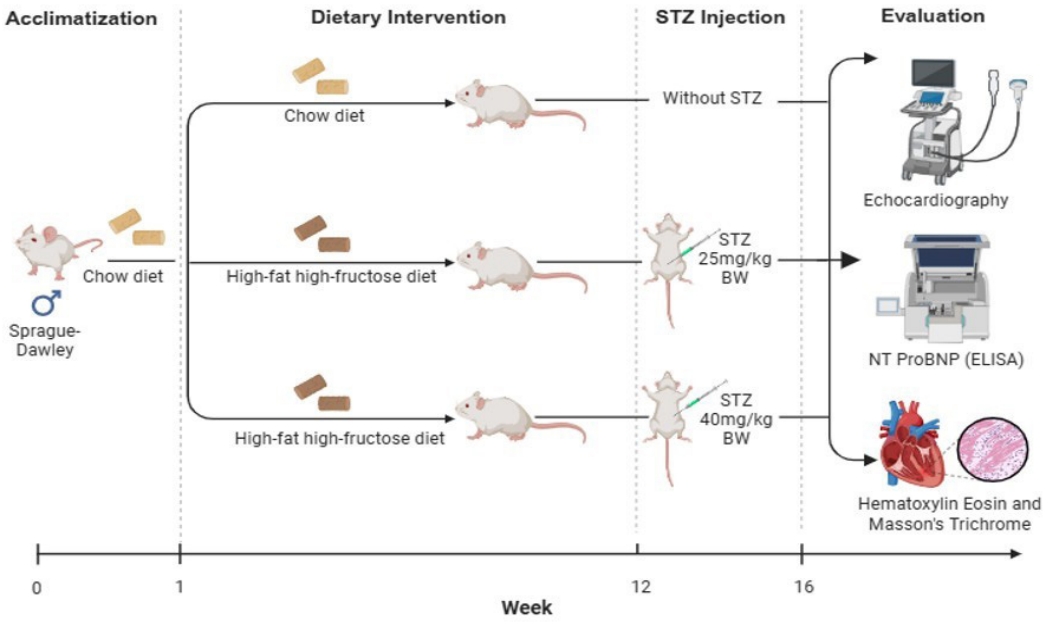


Figure 1. Schematic overview of the study design and experimental timeline.

Evaluation

Echocardiographic Assessment

Cardiac evaluation was performed at week 16 using transthoracic echocardiography. Transthoracic echocardiography was performed under ketamine anesthesia at a dose of 15 mg/kg. Anesthetic depth was adjusted to maintain the heart rate between 300 and 450 x/min during image acquisition. Two veterinarians independently evaluated all measurements and were blinded to the treatment groups. The transducer was positioned in a stationary holder perpendicular to the rat, although manual adjustment was performed when necessary to obtain optimal imaging. Doppler analysis was performed using the Versana Active ultrasound system (GE Healthcare, USA) equipped with a 15-MHz linear array transducer to assess cardiac function.

Parameters assessed included Left Ventricular End-Diastolic Diameter (LVEDD), Left Ventricular End-Systolic Diameter (LVESD), Ejection Fraction (EF), Fractional Shortening (FS), Interventricular Septal Thickness at End-Diastole (IVSd), Left Ventricular Posterior Wall Thickness at End-Diastole (LVPWd), Peak E velocity (E), Early diastolic tissue velocity (e'), Peak A velocity (A), E/e' ratio, and E/A ratio.

Histopathological Examination

Cardiac tissues were processed using graded alcohol dehydration, xylene clearing, and paraffin embedding. Sections of 5 μm thickness were stained with Hematoxylin–Eosin (HE) and Masson's Trichrome (MT) for evaluation of myocardial morphology, fibrosis, hypertrophy, and inflammatory cell infiltration. Histopathological sections were examined under ×200 magnification using a light microscope. For MT assessment, five sections from each heart were evaluated, and the mean percentage of fibrotic involvement across the sections was calculated. Histopathological evaluation was independently performed by two observers who were blinded to the treatment groups.

Biochemical Analysis

Serum samples were obtained by centrifugation at 2500 rpm for 15 minutes and stored at –80 °C. Lipid profile was analyzed using spectrophotometric methods, and NT-proBNP levels were measured using an ELISA method according to the manufacturer's instructions. Serum samples were obtained by centrifugation at 2500 rpm for 15 minutes and stored at –80 °C.

Data Collection

Baseline measurements included body weight, body length, and fasting blood glucose obtained after the acclimatization period. Blood samples were collected from the lateral tail vein, and glucose levels were measured using an enzymatic-based glucometer.

Throughout the study, metabolic parameters were monitored before and after STZ induction. Echocardiographic and histopathological data were recorded systematically and tabulated prior to statistical analysis.

Data Analysis

All collected data were analyzed using IBM SPSS Statistics version 29. Data distribution was assessed using the Shapiro–Wilk test ($n < 50$). Normally distributed data were analyzed using one-way ANOVA, whereas non-normally distributed data were analyzed using the Kruskal–Wallis test. Comparisons between the two groups were conducted using the results of the post hoc Bonferroni test. Variables with p-values < 0.05 were defined as statistically significant.

Results

Metabolic Characteristics

Analysis of body weight showed no significant differences between the three groups, both before and after STZ induction ($p>0.05$). No significant changes in body weight were observed following HFHF administration and STZ induction (Figure 2A).

Analysis of blood glucose levels demonstrated a significant difference between groups after STZ induction ($p<0.05$). Both the 40 mg/kg and 25 mg/kg STZ groups showed significant differences compared with the control group. However, despite the overall significant group effect, pairwise analysis showed no significant difference between the 25 mg/kg and 40 mg/kg STZ groups (Figure 2B).

Lipid profile parameters were evaluated at week 11. The HFHF-treated groups showed significantly higher triglyceride levels compared with the control group ($p < 0.05$). In contrast, Low-Density Lipoprotein (LDL), High-Density Lipoprotein (HDL), and total cholesterol levels showed no significant differences among groups (Figure 2C-F).

Hemodynamic Parameters

No significant differences in heart rate, systolic blood pressure, or diastolic blood pressure were observed among the three groups, either at baseline or after STZ induction (all $p > 0.05$).

At baseline, heart rate as well as systolic and diastolic blood pressure were comparable among the control, STZ 25 mg/kg, and STZ 40 mg/kg groups. Following HFHF feeding and STZ induction, post-intervention heart rate, systolic blood pressure, and diastolic blood pressure remained similar across all groups, with no statistically significant intergroup differences observed (Figure 2G-I).

Cardiac Structure and Function

Echocardiographic evaluation was performed at week 15 of the study to assess cardiac function. No significant differences were observed among the three groups in either systolic or diastolic parameters. Left ventricular evaluation demonstrated no significant differences in LVEDD, LVESD, IVSd, LVPWd, EF, FS, E/A ratio, or E/e' ratio (all $p > 0.05$) (Table 1). Two-dimensional, M-mode, and Doppler echocardiography demonstrated comparable left ventricular geometry and motion across all groups. Systolic function, as reflected by ventricular wall motion and contractility patterns on M-mode imaging, appeared preserved in both STZ-treated groups and did not differ visually from controls (Figure 3).

NT-proBNP levels were also measured at week 15 as a marker of myocardial injury. The STZ 40 mg/kg group showed the highest NT-proBNP levels (1367.6 ± 225.0 pg/mL), followed by the STZ 25 mg/kg group (1121,7 ± 222,5 pg/mL) and the control group (624,3 ± 126,4pg/mL). There was a significant difference among the three groups ($p=0.001$). Post-hoc analysis demonstrated that both the 25 mg/kg and 40 mg/kg STZ groups differed significantly from the control group. However, no significant difference was observed between the 25 mg/kg and 40 mg/kg STZ groups (Figure 4).

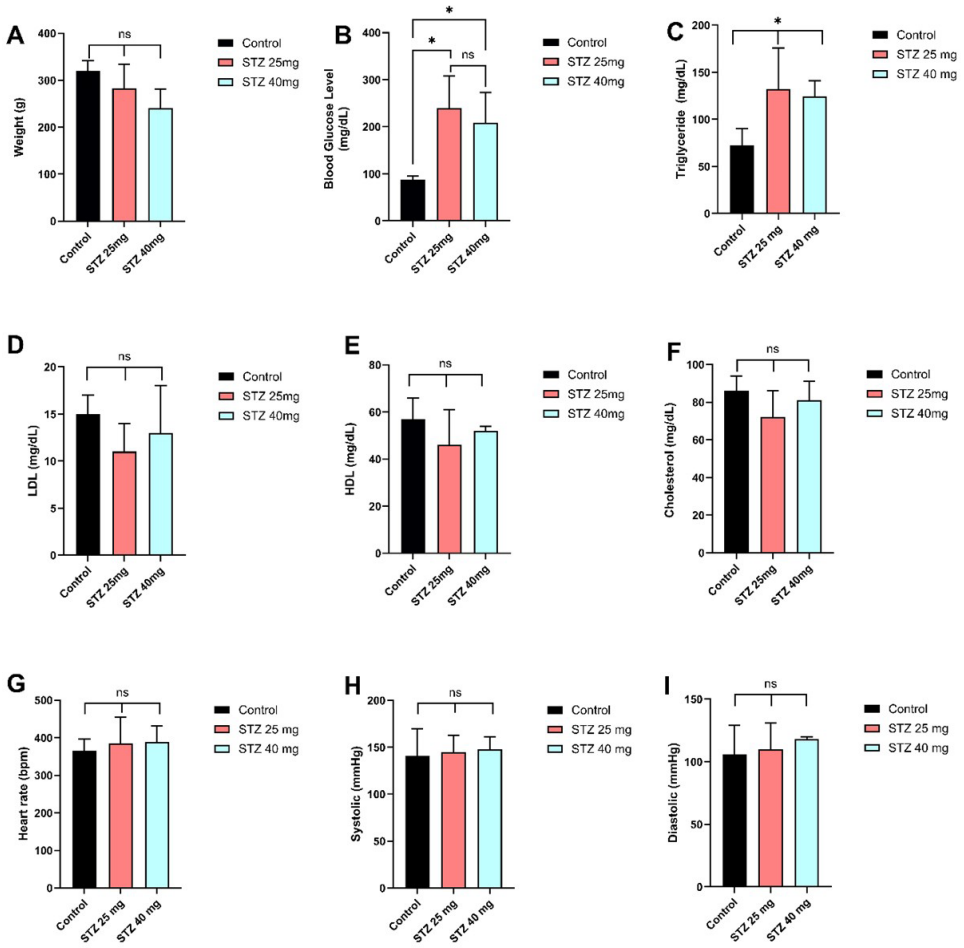


Figure 2. Metabolic and hemodynamic parameters in rats across experimental groups after HFHF feeding and STZ induction. (A) Body weight, (B) blood glucose level, (C) triglyceride level, (D) LDL, (E) HDL, (F) total cholesterol, (G) heart rate, (H) systolic blood pressure, and (I) diastolic blood pressure in the control, STZ 25 mg/kg, and STZ 40 mg/kg groups. All data are presented as mean ± standard deviation. *P < 0.05; ns indicates not significant.

Table 1. Echocardiographic analysis of the three groups.

Parameters	Control	STZ 25 mg	STZ 40 mg	P-value
LVEDD	0.6 ± 0.1	0.7 ± 0.1	0.6 ± 0.03	0.237
LVESD	0.4 ± 0.1	0.4 ± 0.1	0.4 ± 0.1	0.577
IVSd	0.16 ± 0.06	0.13 ± 0.01	0.16 ± 0.01	0.551
LVPWd	0.15 ± 0.05	0.16 ± 0.02	0.15 ± 0.03	0.987
EF	75 ± 10	75 ± 8	77 ± 12	0.976
FS	39 ± 8	40 ± 7	42 ± 13	0.894
Peak E Velocity	0.8 ± 0.06	0.8 ± 0.04	0.7 ± 0.14	0.894
E’	0.04 ± 0.01	0.04 ± 0.01	0.05 ± 0.01	0.816
Peak A Velocity	0.4 ± 0.04	0.5 ± 0.02	0.4 ± 0.07	0.279
E/e’	17.2 ± 1.3	20.4 ± 6.9	16.6 ± 3.3	0.572
E/A	1.9 ± 0.1	1.7 ± 0.1	1.9 ± 0.4	0.429

LVEDD: Left ventricular end-diastolic diameter; LVESD: Left ventricular end-systolic diameter; IVSd: Interventricular septal thickness at end-diastole; LVPWd: Left ventricular posterior wall thickness at end-diastole; EF: Ejection fraction; FS: Fractional shortening; E': Early diastolic mitral annular tissue velocity; E/e': Ratio of early transmitral flow to early diastolic tissue velocity; E/A: Ratio of early to late diastolic transmitral flow.

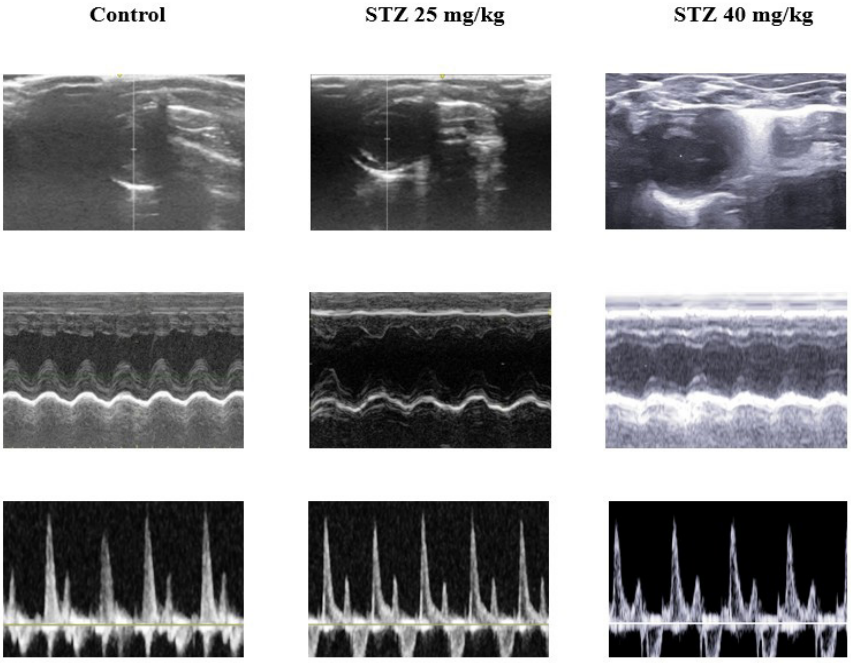


Figure 3. Representative echocardiographic images of systolic and diastolic function for each group. No apparent differences in left ventricular systolic or diastolic performance were observed among the three groups.

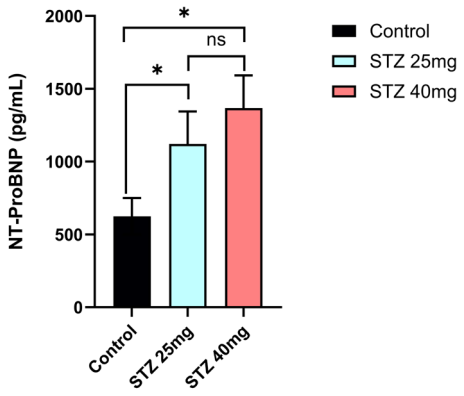


Figure 4. NT-proBNP levels in the control, STZ 25 mg/kg, and STZ 40 mg/kg groups.

Pathological Changes in Myocardium

Cardiac tissue was collected at week 15, and histopathological evaluation was performed using Hematoxylin-Eosin and MT staining (Figure 5). In the control group, cardiomyocytes appeared cylindrical with regular striations and oval-shaped nuclei. A few fibroblasts with more flattened nuclei were also observed between cardiomyocytes. In the HFHF+STZ-treated groups, alterations in myocardial structure were observed. Cardiomyocytes appeared more irregularly arranged, with areas of fiber loss accompanied by inflammatory cell infiltration. In addition, the number of fibroblasts appeared higher than in the control group.

Representative MT–stained sections revealed minimal interstitial collagen deposition in control myocardium, whereas HFHF+STZ-treated groups showed visibly increased collagen accumulation within the interstitial and perivascular regions. Descriptive morphometric assessment of representative Masson's Trichrome-stained sections showed that the collagen-positive area increased from 19.2% in the control group to 38.4% in the STZ 25 mg/kg group and 50.2% in the STZ 40 mg/kg group. These observations are descriptive and based on representative sections.

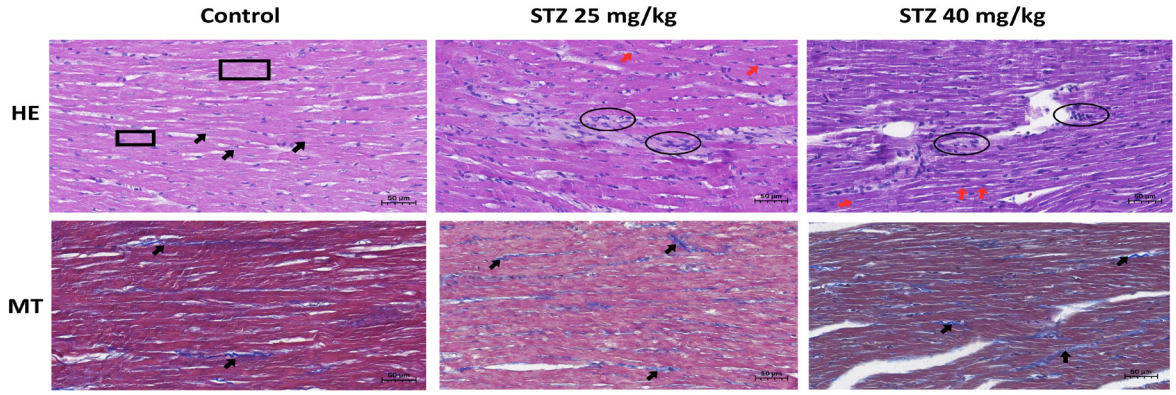


Figure 5. Representative myocardial sections stained with Hematoxylin–Eosin (HE, upper panels) and Masson's Trichrome (MT, lower panels). Representative HE-stained myocardial sections from the control group and STZ-treated groups are shown. The control group demonstrates preserved myocardial architecture with uniformly shaped cardiomyocytes, eosinophilic cytoplasm, visible cross-striations (rectangles), and centrally located oval nuclei (black arrows). In the STZ-treated groups, myocardial architecture shows progressive alterations, including irregular arrangement of cardiomyocytes, variation in cell size and shape, and inflammatory cell infiltration (ovals). Increased numbers of fibroblasts are also observed (red arrows), accompanied by reduced cytoplasmic striations and nuclear changes. (Hematoxylin–Eosin ×200). Representative Masson's Trichrome–stained myocardial sections demonstrate minimal interstitial collagen deposition in the control group, whereas the STZ-treated groups show increased blue-stained collagen within the interstitial and perivascular areas. Representative sections were used for descriptive morphometric assessment of collagen-positive area. Representative sections suggest greater collagen deposition in the STZ 40 mg/kg group than in the STZ 25 mg/kg group. (Masson's Trichrome ×200). All data are presented as mean ± standard deviation. *P < 0.05; ns indicates not significant.

Discussion

This study characterized an early-stage DCM phenotype induced by 12 weeks of exposure to an HFHF diet followed by 2 different doses of STZ. Persistent hyperglycemia, elevated NT-proBNP, and histopathological evidence of myocardial remodeling were observed despite preserved conventional echocardiographic function, consistent with the subclinical stage of DCM. In addition, this study compared two commonly used low-dose STZ regimens to identify an appropriate protocol for reproducing early myocardial remodeling.

Consistent with previous studies, low-dose STZ combined with HFHF feeding in this model produced persistent hyperglycemia without significant weight gain, recapitulating key metabolic features of early-stage T2DM. The metabolic pattern observed showed that the metabolic disturbances were primarily mediated by hyperglycemia. Low-dose STZ causes partial destruction of pancreatic β-cells, resulting in elevated blood glucose levels. This condition, together with metabolic derangement and insulin resistance, reflects the characteristics of type 2 diabetes.[22] In this study, no significant differences in blood glucose levels were observed between the two STZ doses used, indicating that both 25 mg/kg and 40 mg/kg were equally effective in producing a hyperglycemic state.

Our study showed that heart rate and blood pressure remained comparable among groups, indicating preserved systemic hemodynamics. This minimizes confounding effects related to afterload or chronotropic stress, supporting the interpretation that myocardial changes were primarily driven by metabolic disturbances rather than secondary hemodynamic factors.[23] The stability of systemic hemodynamics therefore supports the interpretation that the observed myocardial stress and remodeling signals are more likely attributable to the diabetic metabolic milieu rather than secondary hemodynamic alterations.

Early-stage DCM often manifests only as subtle structural and functional alterations.[24] This study confirms those findings, as NT-proBNP levels showed a significant increase in rats receiving HFHF and STZ. NT-proBNP is a peptide fragment released into the circulation in response to increased wall stress and myocardial remodeling, making it a sensitive early indicator of cardiomyocyte stress.[25] The elevation of NT-proBNP in the absence of changes in echocardiographic parameters suggests the presence of structural alterations that precede functional impairment. The increased NT-proBNP observed in this study indicates ventricular wall stress and myocardial stretch due to structural remodeling, even though cardiac pump function remained preserved. Both 25 mg/kg and 40 mg/kg STZ doses produced significant increases in this biomarker compared with the control group. This finding can be explained by the study of Wen et al.,[20] which demonstrated that functional changes in a rat DCM model were only observed after three months of established diabetes, with structural and ultrastructural alterations occurring earlier.

The absence of overt systolic dysfunction in our echocardiographic assessment should not be interpreted as a lack of myocardial involvement. Experimental evidence from HFD/STZ animal models demonstrates that cardiac remodeling—characterized by collagen deposition, ventricular hypertrophy, and changes in diastolic indices—can precede measurable systolic dysfunction on echocardiography (e.g., preserved EF despite structural changes). In a recent HFD/STZ mouse model, serial echocardiography revealed early diastolic dysfunction with preserved systolic function concurrent with increased fibrosis and remodeling markers, underscoring a temporal dissociation between structural injury and echo functional decline.[26] Similarly, in rodent HFD + STZ models, diastolic impairment has been observed in the absence of systolic dysfunction, while structural changes persist, indicating subclinical disease progression rather than absence of cardiomyopathy.[27]

The present findings should also be interpreted in the context of the study objective, which was to characterize the early stage of DCM rather than advanced heart failure. Although the 32-day observation period after STZ administration was sufficient to demonstrate persistent hyperglycemia, elevated NT-proBNP levels, and histopathological evidence of myocardial remodeling, it may not have been long enough for these structural alterations to progress into overt systolic or diastolic dysfunction detectable by conventional echocardiography. Previous studies have reported that myocardial remodeling precedes functional impairment, with overt echocardiographic abnormalities becoming more evident after a longer duration of diabetes.[16,20] Therefore, extending the observation period in future studies would be valuable to further characterize the temporal progression of this model from early myocardial remodeling to overt cardiac dysfunction.

The structural changes observed were further confirmed through histopathological examination. In our study, myocardial tissue from rats receiving HFHF and STZ exhibited increased fibrosis compared with controls. Several mechanisms have been proposed to explain myocardial injury in diabetes. Excessive production of Reactive Oxygen Species (ROS) combined with reduced radical scavenging capacity of cardiac tissue triggers inflammatory processes and myocardial remodeling.[23,28] We demonstrated that rats with type 2 diabetes exhibited increased inflammatory cell infiltration as well as greater fibrotic tissue deposition. Although histological observations suggested more extensive fibrosis in the 40 mg/kg STZ group, these findings remain descriptive and should be interpreted cautiously due to the limited sample size. Therefore, the 25 mg/kg regimen may provide a more appropriate platform for interventional studies targeting early myocardial remodeling, although this interpretation should be considered exploratory given the descriptive histological assessment and limited sample size.

Chronic hyperglycemia in DM triggers the generation of ROS through the mitochondrial electron transport chain, leading to activation of Poly ADP-Ribose Polymerase (PARP), which directly promotes glycosylation, inhibits phosphoglyceraldehyde dehydrogenase, disrupts

normal glycolytic pathways, and induces further harmful cascades such as increased formation of Advanced Glycation End products (AGEs) and activation of Protein Kinase C (PKC).[14] Persistent hyperglycemia and DCM reduce the expression of Glucose Transporters 1 and 4 (GLUT1 and GLUT4) in cardiomyocytes, resulting in impaired glucose uptake and abnormal myocardial glucose metabolism.[29] Consequently, the myocardium becomes heavily dependent on the oxidation of non-esterified fatty acids as its primary energy source. This metabolic shift promotes the accumulation of lipids and lipid intermediates such as ceramides and diacylglycerol within cardiomyocytes, a condition known as lipotoxicity. Lipotoxicity contributes to impaired myocardial energy supply, increased ROS production, cardiomyocyte necrosis, myocardial fibrosis, and myocardial dysfunction.[29] Glucotoxicity and lipotoxicity arising from altered glucose metabolism further enhance the formation of AGEs in the myocardium, which, together with increased Extracellular Matrix (ECM) protein synthesis, promote collagen accumulation and activation of myocardial fibrosis.[13]

Overall, the findings of this study demonstrate that the combination of HFHF and low-dose STZ reproduced persistent hyperglycemia accompanied by elevated NT-proBNP levels and early histopathological evidence of myocardial remodeling, while conventional echocardiographic function remained preserved. These findings are consistent with an early-stage DCM phenotype and complement previous HFHF-STZ models by providing additional characterization of myocardial remodeling before overt functional impairment develops. Unlike many existing experimental DCM models that primarily capture later-stage disease with overt functional impairment, this model reflects an earlier, subclinical phase of DCM, in which myocardial stress and structural remodeling precede clinically detectable functional decline. This model may therefore serve as a useful experimental platform for investigating early pathogenic mechanisms and evaluating interventions targeting the subclinical stage of DCM.

Study Limitations

Several limitations of this study should be considered when interpreting the findings. First, the sample size was relatively small (n = 4 per group), which may have limited the statistical power to detect subtle differences between groups and reduced the generalizability of the findings. Second, significant changes in cardiac function were not observed on echocardiography, indicating that a longer observation period may be needed to capture progressive functional impairment. Nonetheless, this aligns with the early characteristics of DCM, in which heart failure with preserved EF is more commonly observed than marked reductions in EF during the initial stages of the disease. Furthermore, advanced echocardiographic techniques, such as speckle-tracking or strain imaging, were not performed and may provide more sensitive detection of subclinical myocardial dysfunction. Another limitation of this study is the absence of an HFHF-only group. Consequently, the independent contribution of prolonged HFHF feeding relative to the combined HFHF-STZ protocol could not be directly evaluated. In addition, metabolic parameters such as Homeostatic Model Assessment of Insulin Resistance (HOMA-IR) and Hemoglobin A1c (HbA1c) were not assessed, limiting comprehensive characterization of the diabetic phenotype. Finally, although descriptive morphometric assessment was performed on representative sections, quantitative fibrosis analysis was not conducted in all animals, and additional molecular markers of myocardial fibrosis were not evaluated. Therefore, these findings should be interpreted with caution.

Conclusion

This study demonstrates that the combination of an HFHF diet and low-dose STZ reproduced an early-stage DCM phenotype in Sprague-Dawley rats. The model is characterized by persistent hyperglycemia, elevated NT-proBNP levels as a marker of myocardial stress, and structural histopathological alterations including increased inflammation and fibrosis, while cardiac function on echocardiography remains preserved. Both STZ regimens (25 and 40 mg/kg) produced comparable metabolic and cardiac phenotypes. However, the 25 mg/kg regimen appears to be more suitable for future interventional studies because it reproduced early myocardial remodeling with less extensive structural injury. This model may serve as a foundation for future mechanistic investigations and for testing therapeutic interventions aimed at modifying early myocardial remodeling before progression to more advanced cardiac dysfunction.

List of Abbreviations

A	Peak A velocity
AGEs	Advanced Glycation End products
DCM	Diabetic Cardiomyopathy

DM	Diabetes Mellitus
E	Peak E velocity
e'	Early diastolic tissue velocity
ECM	Extracellular Matrix
EF	Ejection Fraction
FS	Fractional Shortening
GLUT	Glucose Transporters
HbA1c	Hemoglobin A1c
HDL	High-Density Lipoprotein
HE	Hematoxylin–Eosin
HFD	High-Fat Diet
HFHF	High-Fat High-Fructose
HOMA-IR	Homeostatic Model Assessment of Insulin Resistance
LDL	Low-Density Lipoprotein
IVSd	Interventricular Septal Thickness at End-Diastole
LVEDD	Left Ventricular End-Diastolic Diameter
LVESD	Left Ventricular End-Systolic Diameter
LVPWd	Left Ventricular Posterior Wall Thickness at End-Diastole
MT	Masson's Trichrome
NT-proBNP	N-Terminal pro-B-type Natriuretic Peptide
PARP	Poly ADP-Ribose Polymerase
PKC	Protein Kinase C
ROS	Reactive Oxygen Species
STZ	Streptozotocin
T2DM	Type 2 Diabetes Mellitus

Ethical Clearance

The study was approved by the Health Research Ethics Committee of Dr. Cipto Mangunkusumo National General Hospital – Faculty of Medicine, Universitas Indonesia (Approval No. KET-231/UN2.F1/ETIK/PPM.00.02/2025).

Publication Approval

All authors consent to the publication of this manuscript.

Authors' Contributions

Conceptualization, S.A., B.B.S., P.E.W., and N.C.S.; Methodology, S.A. and D.N.; Software, A.K.; Validation, B.S.P., A.K., and F.C.S.; Formal analysis, A.K. and B.S.P.; Investigation, P.E.W., N.C.S., and D.N.; Resources, B.B.S.; Data curation, P.E.W.; Writing—original draft, S.A.; Writing—review and editing, S.A., B.B.S., P.E.W., N.C.S., A.K., F.C.S., B.S.P., and K.E.G.; Visualization, N.C.S., P.E.W., and K.E.G.; Supervision, B.B.S., D.N., and P.E.W.; Project administration, S.A. and B.B.S. All authors have read and agreed to the published version of the manuscript.

Acknowledgments

The authors would like to express their sincere gratitude to the staff of the Animal Research Facility, IMERI, Jakarta, Indonesia, and the Faculty of Medicine, Universitas Indonesia, Jakarta, Indonesia, for their invaluable support and assistance during this study.

Conflict of Interest

The authors declare no conflict of interest.

Availability of Data and Materials

The data presented in this study are available upon reasonable request from the corresponding author.

Funding

This research received no external funding.

Copyright/Permissions for Figures

Not applicable.

Generative AI and AI-Assisted Technologies in the Writing Process

During the preparation of this manuscript, the authors used generative artificial intelligence (AI) tools solely for language editing and improving readability. AI tools were not used to generate scientific data, perform data analysis, or make scientific interpretations. All content was reviewed and verified by the authors, who take full responsibility for the final manuscript.

References

1. Diagnosis and Classification of Diabetes: Standards of Care in Diabetes-2024. Diabetes Care. 2024;47:S20-S42.
2. Five questions on the IDF Diabetes Atlas. Diabetes Res Clin Pract. 2013;102:147-148.

3. RI KK. *Hasil Riset Kesehatan Dasar (Riskesdas) 2018*.; 2018.
4. Fowler MJ. Microvascular and Macrovascular Complications of Diabetes. Clin Diabetes. 2011;29:116-22.
5. Pan Y, Wang Y, Zhao Y, Peng K, Li W, Wang Y, Zhang J, Zhou S, Liu Q, Li X, Cai L, Liang G. Inhibition of JNK phosphorylation by a novel curcumin analog prevents high glucose-induced inflammation and apoptosis in cardiomyocytes and the development of diabetic cardiomyopathy. Diabetes. 2014;63:3497-511.
6. Einarson TR, Acs A, Ludwig C, Panton UH. Prevalence of cardiovascular disease in type 2 diabetes: a systematic literature review of scientific evidence from across the world in 2007-2017. Cardiovasc Diabetol. 2018;17.
7. Rawshani A, Rawshani A, Franzén S, Sattar N, Eliasson B, Svensson A-M, Zethelius B, Miftaraj M, McGuire DK, Rosengren A, Gudbjörnsdottir S. Risk Factors, Mortality, and Cardiovascular Outcomes in Patients with Type 2 Diabetes. N Engl J Med. 2018;379:633-44.
8. Gulsin GS, Athithan L, McCann GP. Diabetic cardiomyopathy: prevalence, determinants and potential treatments. Ther Adv Endocrinol Metab. 2019;10:2042018819834869.
9. National Diabetes Audit 2015-16 Publication Background.
10. Jia G, Hill MA, Sowers JR. Diabetic cardiomyopathy: an update of mechanisms contributing to this clinical entity. Circ Res. 2018;122:624.
11. Zhao X, Liu S, Wang X, Chen Y, Pang P, Yang Q, Lin J, Deng S, Wu S, Fan G, Wang B. Diabetic cardiomyopathy: Clinical phenotype and practice. Front Endocrinol (Lausanne). 2022;13.
12. Avagimyan A, Fogacci F, Pogosova N, Kakrurskiy L, Kogan E, Urazova O, et al. Diabetic Cardiomyopathy: 2023 Update by the International Multidisciplinary Board of Experts. Curr Probl Cardiol. 2024;49.
13. Huo JL, Feng Q, Pan S, Fu WJ, Liu Z, Liu Z. Diabetic cardiomyopathy: Early diagnostic biomarkers, pathogenetic mechanisms, and therapeutic interventions. Cell death Discov. 2023;9.
14. Giri B, Dey S, Das T, Sarkar M, Banerjee J, Dash SK. Chronic hyperglycemia mediated physiological alteration and metabolic distortion leads to organ dysfunction, infection, cancer progression and other pathophysiological consequences: An update on glucose toxicity. Biomed Pharmacother. 2018;107:306-28.
15. Mamuaja MN, Maksum IP, Herlina T, Rumampuk RY. Antidiabetic activities of sesewanua (Clerodendrum squamatum Vahl.) leaves and flavonoids profiling of the bioactive extract. J Plant Interact. 2025;20.
16. Marino F, Salerno N, Scalise M, Salerno L, Torella A, Molinaro C, et al. Streptozotocin-Induced Type 1 and 2 Diabetes Mellitus Mouse Models Show Different Functional, Cellular and Molecular Patterns of Diabetic Cardiomyopathy. Int J Mol Sci. 2023;24.
17. Lee W-S, Kim J. Application of Animal Models in Diabetic Cardiomyopathy. Diabetes Metab J. 2021;45:129-45.
18. Srinivasan K, Ramarao P. Animal models in type 2 diabetes research: An overview. Indian J Med Res. 2007;125.
19. Bugger H, Abel ED. Molecular mechanisms of diabetic cardiomyopathy. Diabetologia. 2014;57:660.
20. Wen W, Cao Y, Chen P, Li J, Li W, Huang G, Zheng H, Zhu X, Zhang H, Chen Y, Huang X, Hu Y, Huang Y. A reliable strategy for establishment of an animal model of diabetic cardiomyopathy: Induction by a high-fat diet combined with single or multiple injections of low-dose streptozotocin. Life Sci. 2024;358:123161.
21. Fuentes-Antras J, Picatoste B, Gomez-Hernandez A, Egido J, Tunon J, Lorenzo O. Updating experimental models of diabetic cardiomyopathy. J Diabetes Res. 2015;2015.
22. Srinivasan K, Ramarao P. Animal models in type 2 diabetes research: an overview. Indian J Med Res. 2007;125:451-72.
23. Bugger H, Abel ED. Molecular mechanisms of diabetic cardiomyopathy. Diabetologia. 2014;57:660-71.
24. Lorenzo-Almorós A, Tuñón J, Orejas M, Cortés M, Egido J, Lorenzo Ó. Diagnostic approaches for diabetic cardiomyopathy. Cardiovasc Diabetol. 2017;16:28.
25. Engle SK, Watson DE. Natriuretic Peptides as Cardiovascular Safety Biomarkers in Rats: Comparison With Blood Pressure, Heart Rate, and Heart Weight. Toxicol Sci. 2016;149:458-72.
26. Karuna N, Kerrigan L, Edgar K, Tonry C, Grieve D, Watson C. Signature of diabetic cardiomyopathy progression using high-fat diet and streptozotocin mouse model: from subclinical to clinical with three-hit mouse model. Eur Heart J. 2024;45.
27. Cohen CD, De Blasio MJ, Lee MKS, Farrugia GE, Prakoso D, Krstevski C, Deo M, Donner DG, Kiriazis H, Flynn MC, Gaynor TL, Mur-

phy AJ, Drummond GR, Pinto AR, Ritchie RH. Diastolic dysfunction in a pre-clinical model of diabetes is associated with changes in the cardiac non-myocyte cellular composition. Cardiovasc Diabetol. 2021;20.
28. Kayama Y, Raaz U, Jagger A, Adam M, Schellinger IN, Sakamoto M, Suzuki H, Toyama K, Spin JM, Tsao PS. Diabetic Cardiovascular Disease Induced by Oxidative Stress. Int J Mol Sci. 2015;16:25234-25263.
29. Isfort M, Stevens SCW, Schaffer S, Jong CJ, Wold LE. Metabolic dysfunction in diabetic cardiomyopathy. Heart Fail Rev. 2014;19:35-48.